

A Novel Method for Identification of Mechanical Properties During Impact Forming of SS 304L Sheet



S. K. Barik , R. Ganesh Narayanan , and N. Sahoo 

Abstract The present investigation focuses to utilize a shock tube facility to perform dynamic forming of a 1-mm-thick SS 304L sheet at an intermediate strain rate. The strain rate evolution is acquired experimentally by mounting a strain rosette on the specimen. During this analysis, the rate-dependent flow stress–strain properties are evaluated at the measured strain rate by the tensile test of the deformed sheet after the shock tube-based experiment. The rate-dependent material properties are identified by testing the deformed tensile sample in the universal testing machine at a crosshead speed of 1 mm/min. The tensile test data of the deformed sheet illustrates that the yield stress and the ultimate tensile stress of the material increase as compared to the results obtained from the base sheet. Moreover, the rate-dependent stress–strain data is validated with the flow stress curve obtained from the Cowper-Symonds flow stress model. Both the flow stress curves demonstrate a good correlation with a slight over prediction. The new method for determining the rate-dependent mechanical properties is reliable and can be implemented in other high strain rate forming processes.

Keywords Shock tube · Tensile test · Strain rate · Impact loading · The flow stress model

1 Introduction

Stainless steel is commonly used in automobile industries because of its good mechanical properties, higher formability and increased resistance to corrosion [1]. Several research activities confirm that during transportation application, the material is exposed to different strain rates in the range of 10^2 – 10^3 [2]. Further, the mechanical properties of the stainless steel are strongly dependent on the loading rates [3]. Thus, it is important to characterize the deformation behaviour of the stainless steel sheets at different strain rates.

S. K. Barik (✉) · R. G. Narayanan · N. Sahoo
Department of Mechanical Engineering, Indian Institute of Technology Guwahati, Assam 781039,
India
e-mail: saibal@iitg.ac.in

Generally, the quasi-static tensile test and the split Hopkinson pressure bar (SHPB) test have been used in most of the investigations to describe the material's mechanical properties at low and high strain rates, respectively. It is difficult to attain intermediate strain rates with the normal test set-up. In the SHPB test set-up, the lowest strain rate of 600 s^{-1} is reported [4]. Recently, Grolleau et al. [5] modified the SHPB into a dynamic bulge testing device and performed a dynamic material test at intermediate strain rates. Further, Ramezani and Ripin [6] conclude that this approach is limited due to strain inhomogeneity because of the increased complexity in the setup.

In the last two decades, high energy rate forming devices have been widely used to obtain the bi-axial forming behaviour of the materials over a wide range of strain rates [7–9]. The shock tube facility has recently been used on a lab scale to study the dynamic response of thin sheets [10–13]. It is generally used to establish an impulsive loading environment for a small duration. The uniformity in loading and ease of handling make the shock tube facility advantageous to utilize as a dynamic testing device. Different levels of shock loading provide different loading conditions that help to study the dynamic mechanical behaviour of the material. Stoffel [10] used a shock tube during the investigation of the dynamic behaviour of the sheet metals. Justusson et al. [11] utilized the shock tube during the bi-axial forming of the aluminium sheets and validated it with the FE model results. Barik et al. [12] investigated the forming behaviour of aluminium alloy sheets using a shock tube and validated the forming outputs to the results obtained from FE simulation. They obtained the rate-dependent material parameters by the tensile test of the sheet deformed using the shock tube and incorporated during FE simulation. The predicted results matched quite well with the experimental outputs.

The tensile test of the deformed sheet is new and reliable to determine the rate-dependent mechanical properties. There has never been an attempt to use the shock tube to acquire the mechanical properties of the SS 304L sheet in the intermediate strain rate range. As a result, the shock tube is used in this study to perform impact loading on SS 304L sheet. During the experiment, a strain rosette is fixed on the sheet to capture the strain evolution during the deformation. The stress–strain data under that strain rate is obtained by the tensile test of the sample cut from the sheet deformed using a shock tube. Further, the tensile test data is validated with the flow stress curve obtained from the Cowper-Symonds model.

2 Experimental Methodology

2.1 Mechanical Properties of the Material

In the current investigation, SS 304L sheet of 1 mm thickness having chemical composition Cr %: 18.20, Ni %: 8.01, Mn %: 1.00, Si %: 0.36, P %: 0.031, C %: 0.056, S %: 0.002 is considered for the analysis. The tensile properties of the base sheet are characterized along 0° , 45° and 90° to the rolling direction in a universal testing

Fig. 1 Engineering stress and strain curves for SS 304L base sheet

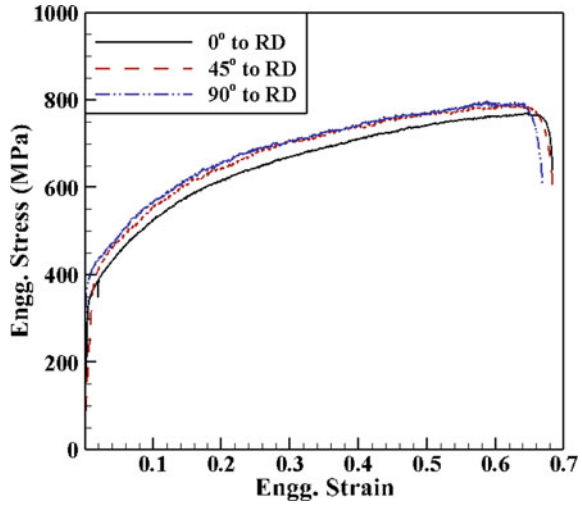


Table 1 Mechanical properties of the base sheet

Material	RD	σ_{ys} (MPa)	σ_u (MPa)	K (MPa)	n	e_u (%)	e_t (%)	r
SS 304L	0°	341 ± 2	746 ± 3	1484 ± 3	0.39	64.8 ± 3.4	68.5 ± 3.2	1.02
	45°	384 ± 3	790 ± 3	1562 ± 3	0.38	61.7 ± 4.8	68.5 ± 4.8	0.99
	90°	378 ± 3	798 ± 4	1498 ± 4	0.36	58.7 ± 3.2	65.4 ± 4.1	0.98

Gauge length: 25 mm; σ_{ys} : Yield stress; σ_u : Ultimate tensile stress; K : Strength coefficient; n : Strain hardening coefficient; r : Plastic strain ratio

machine (UTM) at 1 mm/min crosshead speed as per ASTM-E8 and represented in Fig. 1. ASTM-E517 is used to identify the plastic strain ratios (r) of the sheets. Table 1 depicts the mechanical properties of the base sheet.

2.2 Shock Tube Experiment

In the present investigation, a shock tube facility as illustrated in Fig. 2 has been utilized to perform dynamic loading on sheets. The details about the experimental facility can be found elsewhere [12, 13]. The pressure difference created between the driver and the driven section of the shock tube helps during the sudden rupture of the diaphragm. It generates a shock wave, which propagates at a high velocity towards the end of the shock tube. After imparting the end of the shock tube, the shock wave reflects and generates higher pressure than the incident shock wave. The high-pressure field zone is created inside the shock tube for a short period. This impulsive environment can be used to deform a sheet in bi-axial mode at different strain rates by placing it at the end of the shock tube.

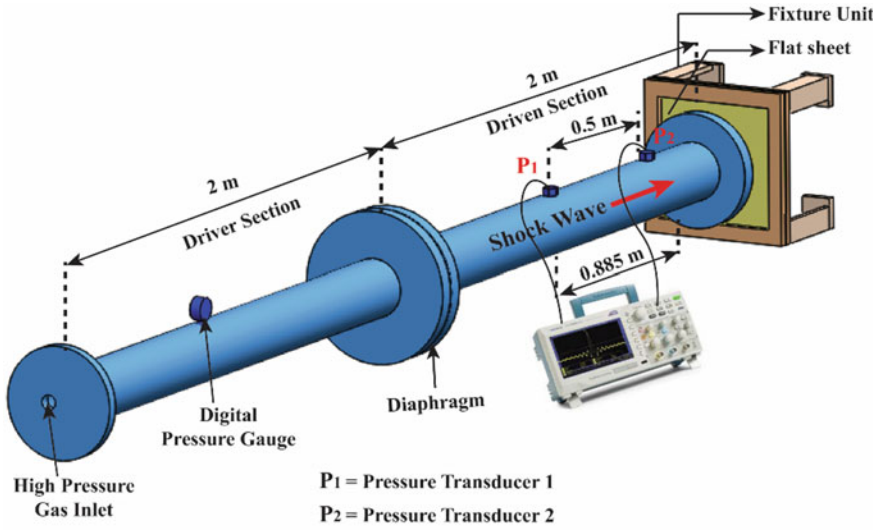
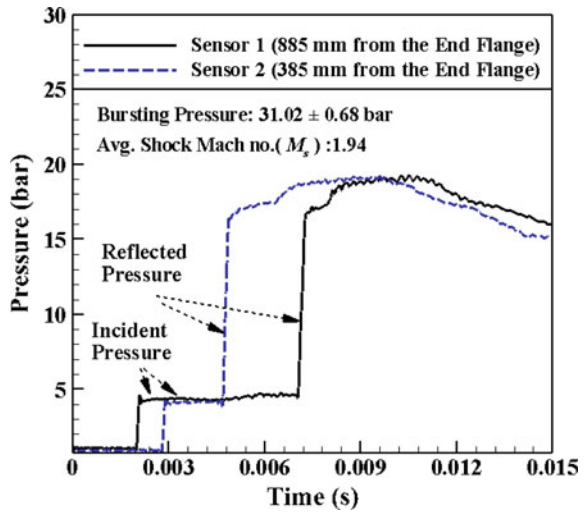


Fig. 2 Illustration of the shock tube experimental facility

During the shock tube experiment, 31.02 ± 0.68 bar of bursting pressure is attained. The detailed instrumentation in the shock tube is mentioned in the previous work of Barik et al. [12]. The pressure–time signals acquired from the pressure transducers positioned in the driven part of the shock tube are illustrated in Fig. 3. The experimentally obtained Mach number (M_s), incident pressure and reflected pressure is 1.94 ± 0.02 , 4.32 ± 0.82 bar and 19.02 ± 0.55 bar, respectively.

Fig. 3 Pressure–time history obtained from the experiment



It is observed that SS 304L becomes rate-dependent when the rate of loading reaches a threshold limit [3]. SHPB has been used in many studies to characterize the mechanical properties of SS 304L sheets at high strain rates [14]. During the high strain rate forming, Cowper-Symonds (CS) flow stress model is also used, which takes into account the rate-dependent effect during material forming. The Cowper-Symonds (CS) flow stress model is given by

$$\sigma = \sigma_{qs} \left(1 + \left(\frac{\dot{\epsilon}}{C_m} \right)^{\frac{1}{P}} \right) \tag{1}$$

where σ_{qs} is the quasi-static constitutive behaviour of the sheet, σ is the dynamic flow stress, $\dot{\epsilon}$ is the effective strain rate, C_m and P are the strain rate factors that scale the material's initial quasi-static stress to represent the dynamic mechanical behaviour. In this study, the dynamic mechanical properties of the sheet are identified by the tensile test of the sheet deformed using a shock tube. The tensile sample is cut from the deformed sheet's mid location along 0° to the RD (Fig. 4), and then it is tested in UTM at 1 mm/min crosshead speed.

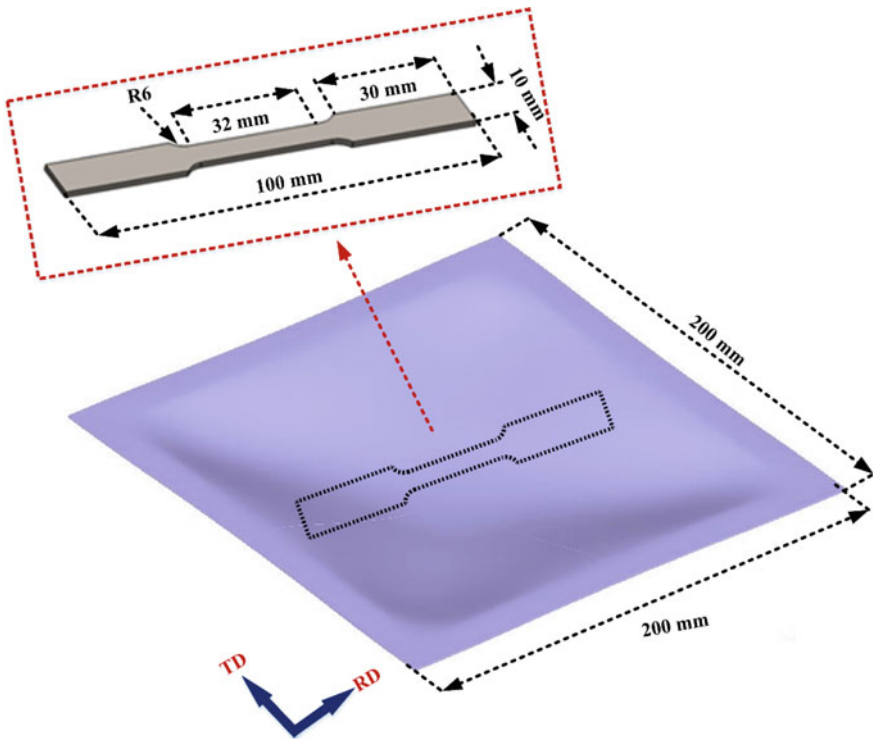


Fig. 4 Tensile test sample obtained from the sheet deformed using the shock tube

2.3 Strain Rate Evolution Measurement

During this study, the strain rosette is used to measure the strain rate evolution during the shock wave-based deformation analysis. Generally, in many high strain rate forming experiments, a high-speed 3D digital image correlation (DIC) system has been utilized to determine the transient variation of the forming parameters [11]. However, it is witnessed that the strain gauge can also be used to measure the strain rate and the results have a good agreement with the results obtained from DIC [15]. Thus, a strain rosette is attached at the centre of the sheet (Fig. 5) to quantify the in-plane strain as well as strain rate along 0° , 45° and 90° to the RD. Details about the strain rosette can be found elsewhere [12]. The strain rosette is connected by the Wheatstone quarter bridge circuit (Fig. 5). When the pressure developed by the shock wave generates impact loading on the sheet, the strain gauge's resistance changes and it causes instability in the Wheatstone bridge.

The output voltage from the Wheatstone bridge circuit is obtained in millivolts. It is difficult to predict the strain outputs from the measured signal. Thus, the voltage outputs are amplified in INA 128, DC voltage amplifier and then captured in an oscilloscope. The voltage outputs can be converted into strain rate signals. The strain rate signals obtained from the strain rosette along 0° , 45° and 90° to the rolling direction are represented in Fig. 6. The effective strain rate ($\dot{\bar{\epsilon}}$) can be obtained using Hill's 1948 yield criterion [16], which takes into account the peak strain rate along 0° and 90° during the calculation. Hill's 1948 yield criterion is expressed as

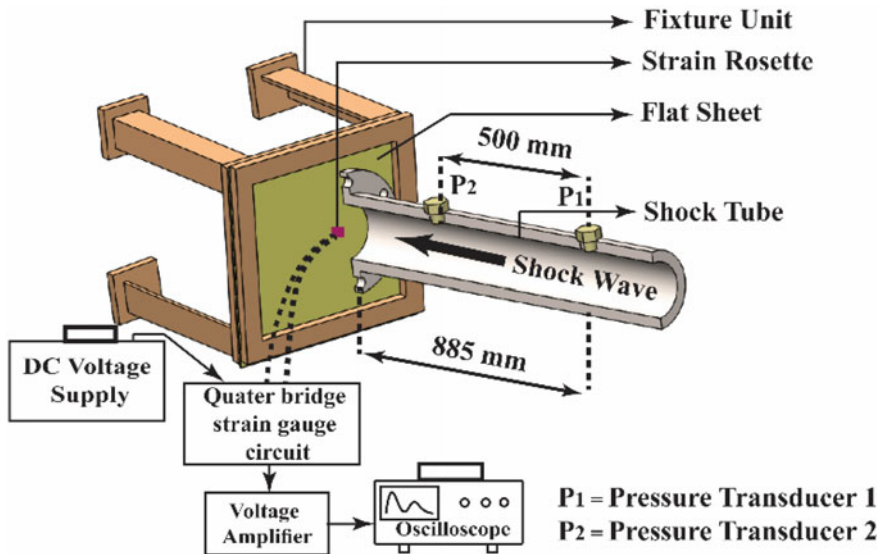
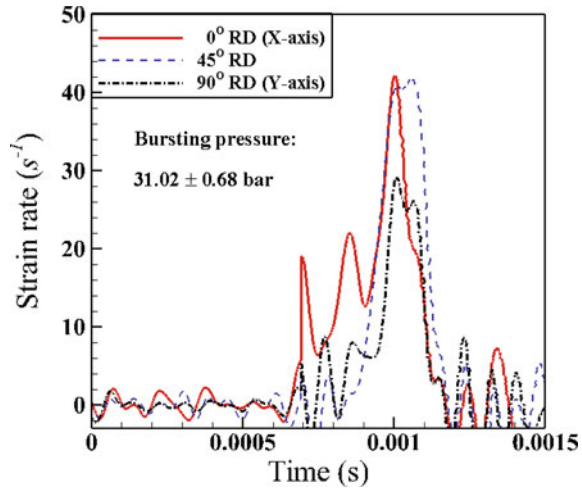


Fig. 5 Strain gauge mounted on the specimen during the experiment

Fig. 6 Strain rate developed during the shock tube-based forming of flat sheet



$$\dot{\bar{\epsilon}}^2 = \frac{(G + H)}{(FG + FH + GH)^2} [F^2(G + H)\dot{\epsilon}_1^2 + G^2(F + H)\dot{\epsilon}_2^2 + H^2(F + G)\dot{\epsilon}_3^2] \quad (2)$$

where $\dot{\bar{\epsilon}}$ is the effective strain rate, $\dot{\epsilon}_1$ is the strain rate along 0° to RD, $\dot{\epsilon}_2$ is the strain rate along 90°, and $\dot{\epsilon}_3$ is the strain rate along the thickness direction. Identification of $\dot{\epsilon}_3$ is difficult, and it is neglected during $\dot{\bar{\epsilon}}$ calculation. Hill's constant (F , G and H) can be correlated to the plastic anisotropy parameters (r_0 and r_{90}) by the relations $F = r_0$; $G = r_{90}$; $H = r_0 r_{90}$ [16]. The values of r_0 and r_{90} are identified experimentally as mentioned in Table 1. The effective strain rate ($\dot{\bar{\epsilon}}$) calculated experimentally is 34.26 s^{-1} .

3 Results and Discussion

3.1 Determination of Rate-Dependent Mechanical Properties

The tensile test results obtained from the deformed sheet are compared to the base sheet (Fig. 7). Table 2 depicts the mechanical properties of the deformed sheet. It is observed that both the yield stress and the ultimate tensile stress of the material rise as compared to the base sheet. The material's strength coefficient (K) increases significantly as a result of the action of strain hardening. However, after the deformation, the strain hardening coefficient (n) does not vary as much.

Furthermore, the identified rate-dependent tensile properties are validated with the dynamic stress–strain curve obtained from the CS model. During the calculation, the quasi-static flow stress data (σ_{qs}) obtained from the base sheet along 0° to RD

Fig. 7 Comparison of the stress–strain curves obtained from the deformed sheet to the Cowper-Symonds model

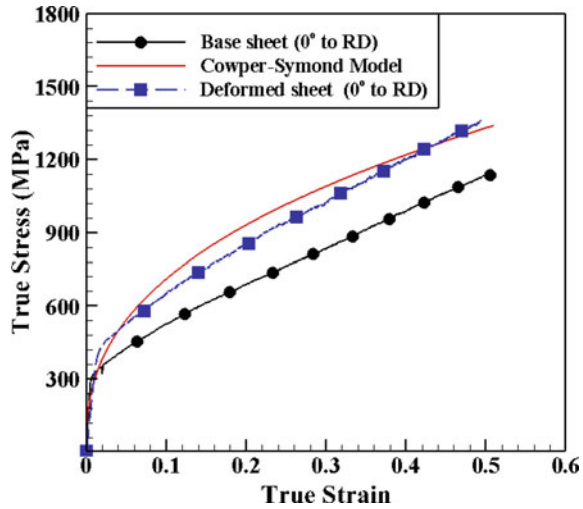


Table 2 Comparison of tensile properties of the deformed sheet with the base sheet

Tensile properties (0° to RD)	Base sheet	Deformed sheet
σ_{ys} (MPa)	341 ± 2	386 ± 3
σ_u (MPa)	746 ± 3	828 ± 3
n	0.39	0.39
K	1484 ± 3	1730 ± 5

is considered. The values of $C_m = 17,772 \text{ s}^{-1}$ and $P = 3.16$ for SS 304L sheets are obtained from literature [17]. The effective strain rate ($\dot{\epsilon}$) of deformation is calculated experimentally as 34.26 s^{-1} (reported in Sect. 2.3). The results illustrate that rate-dependent flow stress data obtained from the CS model slightly deviated from the data obtained from the tensile test of the deformed sheet. The correlation coefficient (R) between both the flow stress curves is obtained as 0.963, which is an acceptable limit. It confirms that the approach of obtaining the dynamic mechanical properties by the tensile test of the deformed sheets is reliable and can be used to predict the dynamic forming behaviour of the sheet. A similar approach can be implemented in another rate-dependent forming processes to identify the rate-dependent mechanical properties.

4 Conclusions

The present work aims to identify the rate-dependent mechanical properties of a 1-mm-thick SS 304L sheet. For this analysis, a tensile sample is cut from the mid

location of the sheet deformed using the shock tube and tested in UTM. The rate-dependent flow stress–strain data is also validated with the Cowper-Symonds flow stress model. The following conclusions are drawn from the results.

- i. The tensile test data obtained from the deformed sheet has a reasonable correlation with the Cowper-Symonds model. Thus, the same procedure can be followed during the identification of mechanical properties in other high strain rate forming processes.
- ii. The yield strength and ultimate tensile strength obtained from the deformed sheet are higher than the base sheet. The strength coefficient (K) of the material raises significantly after deformation because of the strain hardening phenomenon. However, there is less variation in the strain hardening coefficient.
- iii. During the shock tube-based experiment, the strain rosette can able to acquire the strain rate of deformation. The peak strain rate confirms the rate of loading during the experiment.

References

1. Campos HB, Butuc MC, Gracio JJ, Rocha JE, Duarte JM (2006) Theoretical and experimental determination of the forming limit diagram for the AISI 304 stainless steel. *J Mater Process Technol* 179:56–60. <https://doi.org/10.1016/j.jmatprotec.2006.03.065>
2. Vaz-Romero A, Rodríguez-Martínez JA, Arias A (2015) The deterministic nature of the fracture location in the dynamic tensile testing of steel sheets. *Int J Impact Eng* 86:318–335. <https://doi.org/10.1016/j.ijimpeng.2015.08.005>
3. Rodríguez-Martínez JA, Pesci R, Rusinek A (2011) Experimental study on the martensitic transformation in AISI 304 steel sheets subjected to tension under wide ranges of strain rate at room temperature. *Mater Sci Eng A* 528(18):5974–5982. <https://doi.org/10.1016/j.msea.2011.04.030>
4. Smerd R, Winkler S, Salisbury C, Worswick M, Lloyd D, Finn M (2006) High strain rate tensile testing of automotive aluminium alloy sheet. *Int J Impact Eng* 32(1–4):541–560. <https://doi.org/10.1016/j.ijimpeng.2005.04.013>
5. Grolleau V, Gary G, Mohr D (2008) Biaxial testing of sheet materials at high strain rates using viscoelastic bars. *Exp Mech* 48(3):293–306. <https://doi.org/10.1007/s11340-007-9073-5>
6. Ramezani M, Ripin ZM (2010) Combined experimental and numerical analysis of bulge test at high strain rates using split Hopkinson pressure bar apparatus. *J Mater Process Technol* 210(8):1061–1069. <https://doi.org/10.1016/j.jmatprotec.2010.02.016>
7. Oliveira DA, Worswick MJ, Finn M, Newman D (2005) Electromagnetic forming of aluminium alloy sheet: Free-form and cavity fill experiments and model. *J Mater Process Technol* 170(1–2):350–362. <https://doi.org/10.1016/j.jmatprotec.2005.04.118>
8. Dariani BM, Liaghat GH, Gerdooei M (2009) Experimental investigation of sheet metal formability under various strain rates. *Proc Inst Mech Eng Part B J Eng Manuf* 223(6):703–712. <https://doi.org/10.1243/09544054JEM1430>
9. Balanethiram, V. S., Daehn, G. S. (1992). Enhanced formability of interstitial free iron at high strain rates. *Scripta Metallurgica et Materialia* 27(12):1783–1788. [https://doi.org/10.1016/0956-716X\(92\)90019-B](https://doi.org/10.1016/0956-716X(92)90019-B)
10. Stoffel M (2004) Evolution of plastic zones in dynamically loaded plates using different elastic-viscoplastic laws. *Int J Solids Struct* 41(24–25):6813–6830. <https://doi.org/10.1016/j.ijsolstr.2004.05.060>

11. Justusson B, Pankow M, Heinrich C, Rudolph M, Waas AM (2013) Use of a shock tube to determine the bi-axial yield of an aluminium alloy under high rates. *Int J Impact Eng* 58:55–65. <https://doi.org/10.1016/j.ijimpeng.2013.01.012>
12. Barik SK, Narayanan RG, Sahoo N (2020) Prediction of Forming of AA 5052–H32 Sheets under Impact Loading and Experimental Validation. *J Mater Eng Perform* 29:3941–3960. <https://doi.org/10.1007/s11665-020-04884-w>
13. Barik SK, Narayanan RG, Sahoo N (2020) Forming response of AA5052–H32 sheet deformed using a shock tube. *Trans Nonferrous Met Soc China* 30:603–618. [https://doi.org/10.1016/S1003-6326\(20\)65239-6](https://doi.org/10.1016/S1003-6326(20)65239-6)
14. Jin H, Sanborn B, Lu WY, Song B (2021) Mechanical characterization of 304L-VAR stainless steel in tension with a full coverage of low, intermediate, and high strain rates. *Mech Mater* 152:103654. <https://doi.org/10.1016/j.mechmat.2020.103654>
15. Louar MA, Belkassam B, Ousji H, Spranghers K, Kakogiannis D, Pyl L, Vantomme J (2015) Explosive driven shock tube loading of aluminium plates: experimental study. *Int J Impact Eng* 86:111–123. <https://doi.org/10.1016/j.ijimpeng.2015.07.013>
16. Wagoner RH, Chenot JL (1996) *Fundamentals of metal forming*. John Wiley & Sons Inc., New York
17. Mancini E, Campana F, Sasso M, Newaz G (2012) Effects of cold rolling process variables on final surface quality of stainless steel thin strip. *Int J Adv Manuf Technol* 61:63–72. <https://doi.org/10.1007/s00170-011-3698-3>